buildings

Article

Effect of Rock Mass Disturbance on Stability of 3D Hoek–Brown Slope and Charts

Jingshu Xu [1], Xinrui Wang [1], Pengfei Xie [1], Ruotong Wang [1] and Dianchun Du [2,*]

[1] Faculty of Architecture, Civil and Transportation Engineering, Beijing University of Technology, Beijing 100124, China
[2] Key Laboratory of Concrete and Prestressed Concrete Structures of Ministry of Education, Southeast University, Nanjing 211102, China
* Correspondence: dudianchun@seu.edu.cn

Abstract: The present study performs a stability analysis of a three-dimensional (3D) rock slope in disturbed rock masses following the Generalized Hoek–Brown (GHB) failure criterion. The factor of safety (*FoS*) of the slope is derived and the optimal solution is captured combining the limit analysis method and the strength reduction technique. It is indicated by the parametric analysis that the 3D geometric characteristics have a significant impact on slope stability such that *FoS* decreases sharply with the increase in the width-to-height ratio B/H within $0 < B/H \leq 2.0$ and thereafter reaches a constant value asymptotically. The *FoS* decreases more than 60% linearly when the disturbance factor D increases from 0 to 1.0. Stability charts and slope angle weight factor f_{β_3D} for 3D slopes are proposed to provide a convenient and straightforward approach to obtain the *FoS* solutions of 3D slopes. A case study was carried out to apply the stability charts on practical engineering cases, which showed that slope stability under two-dimensional (2D) plane strain will lead to conservative results, and a 3D stability analysis of slope is more appropriate, especially for a slope with a limited width.

Keywords: generalized Hoek–Brown failure criterion; 3D slope; disturbed rock mass; stability charts; slope angle weighting factor

check for updates

Citation: Xu, J.; Wang, X.; Xie, P.; Wang, R.; Du, D. Effect of Rock Mass Disturbance on Stability of 3D Hoek–Brown Slope and Charts. *Buildings* **2024**, *14*, 114. https://doi.org/10.3390/buildings14010114

Academic Editor: Yi Xue

Received: 20 October 2023
Revised: 24 December 2023
Accepted: 29 December 2023
Published: 31 December 2023

Copyright: © 2023 by the authors. Licensee MDPI, Basel, Switzerland. This article is an open access article distributed under the terms and conditions of the Creative Commons Attribution (CC BY) license (https://creativecommons.org/licenses/by/4.0/).

1. Introduction

Determining the factor of safety (*FoS*) is a significant issue in geotechnical engineering to estimate the stability of slopes in rock masses such as dams and open pit excavations. Due to its theorical and practical significance, this classical issue has attracted plenty of attention, and it was found that the well-known Mohr–Coulomb failure criterion can-not reflect the nonlinear strength characteristics of rock masses. To address this issue, the Generalized Hoek–Brown (GHB) failure criterion was proposed by Hoek and Brown [1] and Hoek et al. [2] to describe the strength of rock masses and has been widely accepted and employed to investigate strength properties of rock masses and rock slope stability.

Due to its nonlinearity, it is not convenient to apply the Generalized Hoek–Brown failure criterion directly on stability analysis of geotechnical structures. To solve this issue, the generalized tangent approach [3–5] and the equivalent Mohr–Coulomb strength parameters method [2,6–8] were proposed, respectively, to determine the shear strength of rock masses and, consequently, to introduce the Generalized Hoek–Brown failure criterion into slope stability analysis. Based on the generalized tangent approach, the Generalized Hoek–Brown failure criterion was used by Yang [3] to investigate the stability of a 3D slope subjected to pore water pressure. Analytical expression of the stability number was derived and the influences of factors such as pore water pressure and slope geometry on slope stability were investigated. Pan et al. [4] employed the limit analysis method and the response surface method to conduct a probabilistic stability analysis of a 3D rock slope following the Generalized Hoek–Brown failure criterion. The impacts of uncertainty level and correlation relationships of related parameters and distribution types on probabilistic stability of a rock slope were discussed, and a set of designed charts were also proposed. Qin et al. [5] performed a stability analysis of a pile-reinforced slope in fractured rock mass subjected to pore water pressure, analytical expressions of the lateral force of piles and surcharge loading on slope crest were derived, and a parametric study was also conducted to investigate the effects of strength parameters and pile location on slope stability. Based on the equivalent Mohr–Coulomb strength parameters method, Li et al. [6,7] proposed a series of (seismic) stability charts to estimate *FoS* solutions of rock slopes. The formula proposed by Hoek et al. [2] was also modified by Li et al. [6] to estimate equivalent Mohr–Coulomb strength parameters for rock masses in slopes. Xu and Yang [8] investigated the 3D seismic stability of a rock slope in Hoek–Brown media, where a set of seismic stability charts were proposed and applied on practical cases.

In addition, combining the limit analysis method with numerical software, Saada et al. [9] conducted a stability analysis of rock slope subjected to seepage forces in Hoek–Brown media, where the effects of strength parameters and seepage forces on slope stability were analyzed. A set of seismic stability charts of a 30° slope was proposed by Jiang et al. [10], and a convenient calculation method to solve the *FoS* of slopes was also established in virtue of the proposed charts. Shen et al. [11] and Sun et al. [12] performed chart-based stability analysis of slope, respectively, to propose stability charts to calculate *FoS* solutions of a 45° slope in undisturbed rock mass. Expressions of the slope angle weighting factor f_β and the disturbance factor f_D were thereafter proposed to estimate the *FoS* solutions of slope with different slope angles under various disturbance factors. Li et al. [13,14] conducted (seismic) stability analysis of slope in both homogeneous and inhomogeneous disturbed rock masses, where a set of stability charts was proposed to estimate the *FoS* of slopes in disturbed rock masses. More recently, a series of failure mechanisms was proposed by Park and Michalowski [15–17] to introduce nonlinear strength criteria directly to stability analysis of rock slopes. Thereafter, a seismic stability analysis in rock slopes was conducted by Xu and Du [18] to propose a series of seismic stability charts. Probabilistic analyses for 3D slopes were conducted by Hu and Sun et al. [19,20] to investigate the related parameters on the stability of rock slopes.

Even though many efforts have been devoted to investigate stability of slopes in rock masses, the aforementioned investigations were mainly conducted under 2D plane strain. However, it has been proved that the 3D characteristics of slope has crucial impacts on stability and the *FoS* solutions of slopes [21–23]. The problem of stability of 3D slope in disturbed rock masses still presents a significant challenge to designers. In this view, an issue, which has both theoretical importance and practical significance, is raised: How can we investigate the stability of 3D rock slope in disturbed rock masses? How can we propose a convenient and straightforward approach to obtain the *FOS* of slopes in disturbed rock mass?

From this point of view, the present study conducts a stability analysis of 3D slope in disturbed rock masses. The equivalent Mohr–Coulomb strength parameters method is employed to introduce the Generalized Hoek–Brown failure criterion into slope stability analysis. Expression of the *FoS* of a slope is derived by combining the upper bound theorem of limit analysis and the strength reduction technique, and a comparison is made to verify the validity of the present study. A parametric analysis is conducted to investigate the effects of rock mass disturbance on slope stability, and a set of stability charts and estimating equations to solve the slope angle weighting factor f_{β_3D} are proposed to provide a convenient and straightforward approach to obtain the *FoS* of slopes in disturbed rock masses. A case study was carried out and is detailed at the bottom of the present paper to apply the presented stability charts on practical engineering issues, and it was found that a 3D stability analysis of slope is more appropriate, especially for slopes with limited widths.

2. The Generalized Hoek–Brown Failure Criterion and Its Applicability

2.1. The Generalized Hoek–Brown Failure Criterion

The Generalized Hoek–Brown failure criterion presented by Hoek and Brown [1] and Hoek et al. [2] is expressed as follows:

$$\sigma_1 = \sigma_3 + \sigma_{\text{ci}}(m_b\sigma_3/\sigma_{\text{ci}} + S)^{\alpha} \tag{1}$$

where σ_1 denotes the maximum principal stress, σ_3 denotes the minimum principal stress, and σ_{ci} denotes the uniaxial compressive strength of rock material. m_b, S, and α are expressed as follows:

$$m_b = m_{\text{i}} \exp\left(\frac{GSI - 100}{28 - 14D}\right) \tag{2}$$

$$S = \exp\left(\frac{GSI - 100}{9 - 3D}\right) \tag{3}$$

$$\alpha = \frac{1}{2} + \frac{1}{6}\left[\exp\left(-\frac{GSI}{15}\right) - \exp\left(-\frac{20}{3}\right)\right] \tag{4}$$

where GSI $(5 \leq GSI \leq 100)$ denotes the geological strength index; m_i $(1 \leq m_i \leq 35)$ denotes the index representing stiffness of rock mass; and D $(0 \leq D \leq 1.0)$ denotes the disturbance factor of the rock material, which is 0 for undisturbed rock mass and 1.0 for disturbed rock mass [9,11,24–26].

As illustrated in Figure 1, rock masses can be classified into three groups, i.e., Group I is the isotropic intact rock masses, Group II is the extremely anisotropic rock mass, and Group III is the heavily jointed rock masses. In the present study [6,8], the rock masses are assumed to be either in Group I or Group III, making the rock masses being dealt with in the present study isotropic and suiting the Generalized Hoek–Brown failure criterion.

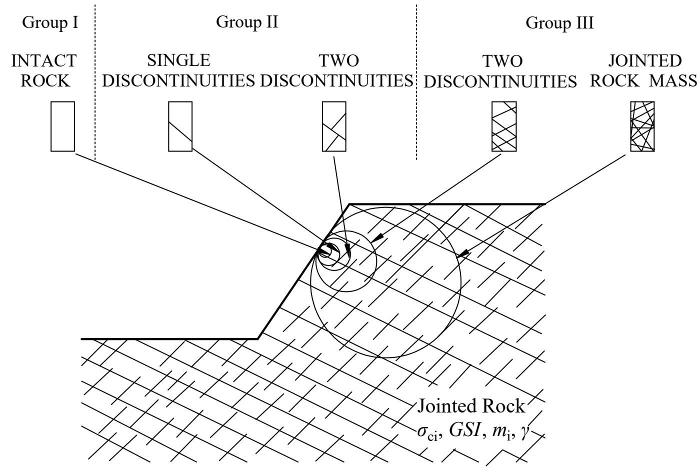

Figure 1. Classification of rock masses adopted from Li et al. [6].

2.2. The Equivalent Mohr–Coulomb Strength Parameters Method

Due to its nonlinearity, the Generalized Hoek–Brown failure criterion is not convenient for direct application on slope stability analysis. Consequently, the equivalent Mohr–Coulomb parameters method was proposed by Hoek et al. [2]. By curve fitting to apply the Hoek–Brown failure criterion on slope stability analysis, as shown in Figure 2, it is seen that the straight equivalent Mohr–Coulomb envelope cannot fit the Hoek–Brown curve entirely and that the stress space is divided into three regions. The shear strength parameters are considered approximately equal to the Generalized Hoek–Brown failure criterion in Region 2.

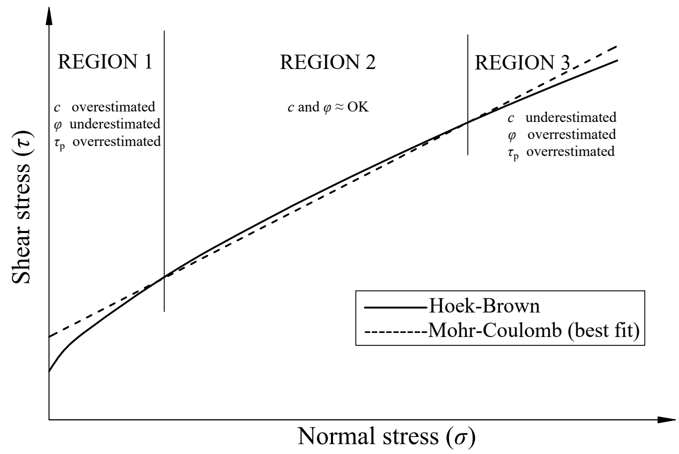

Figure 2. Generalized Hoek–Brown failure criterion and its fitting curve from Li et al. [6].

The equivalent Mohr–Coulomb parameters c and φ read

$$c = \frac{\sigma_{\text{ci}}[(1+2\alpha)S + (1-\alpha)m_b\sigma'_{3n}](S + m_b\sigma'_{3n})^{\alpha-1}}{(1+\alpha)(2+\alpha)\sqrt{1 + \left[6m_b\alpha(S + m\sigma'_{3n})^{\alpha-1}\right]/(1+\alpha)(2+\alpha)}} \tag{5}$$

$$\varphi = \arcsin\left[\frac{6m_b\alpha(S + m\sigma'_{3n})^{\alpha-1}}{2(1+\alpha)(2+\alpha) + 6m_b\alpha(s + m_b\sigma'_{3n})^{\alpha-1}}\right] \tag{6}$$

where $\sigma'_{3n} = \sigma'_{3\max}/\sigma_{ci}$. As suggested by Hoek et al. [2], the maximum confining pressure $\sigma'_{3\max}$ can be calculated as

$$\frac{\sigma'_{3\max}}{\sigma'_{\text{cm}}} = 0.72\left[\frac{\sigma'_{\text{cm}}}{\gamma H}\right]^{-0.91} \tag{7}$$

$$\sigma'_{\text{cm}} = \sigma_{\text{ci}}\frac{[m_b + 4S - \alpha(m_b - 8S)](m_b/4 + S)^{\alpha-1}}{2(1+\alpha)(2+\alpha)} \tag{8}$$

where σ'_{cm} denotes the compressive strength of rock masses, and γ and H denote the unit weight of rock mass and slope height, respectively. More recently, Li et al. [6] found that the equivalent parameters c and φ derived based on Equation (7) will lead to unconservative estimations of slope stability. New equations proposed by Li et al. [6] are expressed as follows:

$$\frac{\sigma'_{3\max}}{\sigma'_{\text{cm}}} = 0.41\left[\frac{\sigma'_{\text{cm}}}{\gamma H}\right]^{-1.23} \quad (\text{gentle slope, } \beta < 45^\circ) \tag{9}$$

$$\frac{\sigma'_{3\max}}{\sigma'_{\text{cm}}} = 0.2\left[\frac{\sigma'_{\text{cm}}}{\gamma H}\right]^{-1.07} \quad (\text{steep slope, } \beta \geq 45^\circ) \tag{10}$$

where β is the slope angle. In the present study, the equivalent Mohr–Coulomb strength parameters obtained based on Equations (9) and (10) are employed to perform the present slope stability analysis.

3. The Kinematic Approach of Limit Analysis

The kinematic approach of limit analysis, an effective methodology to analyze the stability of geotechnical structures, is employed in this work to investigate the stability of a 3D slope in disturbed rock mass. This approach states that the internal work rate is no less than the external work rates, as follows:

$$\int_V \sigma^*{}_{ij}\dot{\varepsilon}^*{}_{ij}dV \geq \int_S T_i v_i dS + \int_V X_i v_i^* dV \tag{11}$$

where ${\sigma^*}_{ij}$ and ${\dot{\varepsilon}^*}_{ij}$ are the stress and the strain rate, respectively; v_i and v_i^* are the velocities along the failure surface and in the kinematically admissible mechanism, respectively; and S and V are the boundary and volume of the slope, respectively.

4. Slope Stability Analysis Using Limit Analysis

4.1. Failure Mechanism of a 3D Slope

The three-dimensional (3D) failure mechanism of slope in the framework of the upper bound theorem of limit analysis is illustrated in Figure 3. Figure 3a illustrates half of the failure mechanism of a 3D slope, which comprises the 3D horn section (Figure 3b) and the insert plane. The 3D horn failure mechanism illustrated in Figure 3b has the boundary of two logarithmic spiral curves AC and $A'C'$, of which AC is also the failure surface of slope. The initial and terminate rotating angle are r_0 and r_h, respectively. From the geometrical relationship in Figure 3, the factor of safety (*FoS*) solution of a 3D slope is determined by four variables: θ_0, θ_h, the ratio ${r'}_0/r_0$, and b/H, as illustrated in Figure 3. A detailed description about the 3D failure mechanism can be found in the reports of Michalowski [21] and Xu and Yang [8].

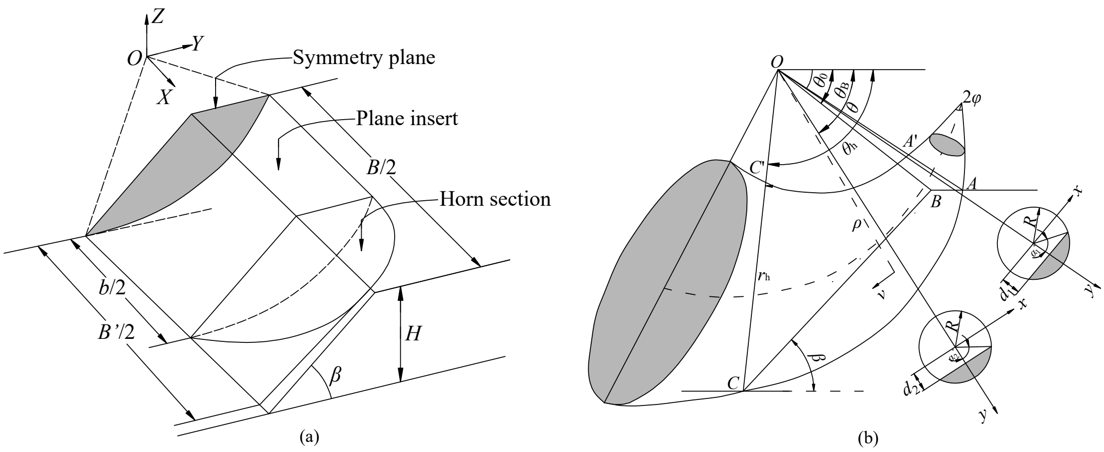

Figure 3. Failure mechanism of slope (**a**) with plane insert and (**b**) 3D horn failure mechanism.

4.2. FoS Solution of Slope

Based on the upper bound theorem of limit analysis, the external work rate by rock masses weight W_γ can be expressed as follows:

$$W_\gamma = \int\limits_V \gamma v \cos\theta dV \tag{12}$$

where γ is the unit weight of rock mass; $v = \omega\rho$ is the velocity magnitude; θ is the angle between a rotational radius r and the horizontal line, as illustrated in Figure 3b; and V is the volume of the failure block. The infinitesimal volume element dv can be calculated as follows:

$$dV = \rho\sqrt{R^2 - (\rho - r_c)^2} d\rho d\theta \tag{13}$$

The expression of the external work rate by the weight of the failure block can be expressed as follows:

$$W_\gamma = \omega\gamma \int_{\theta_0}^{\theta_h} \int_{r_s}^{r} \rho^2 \left[2\sqrt{R^2 - (\rho - r_c)^2} + b\right] \cos\theta d\rho d\theta \tag{14}$$

where $r_s = \begin{cases} r_0 \frac{\sin\theta_0}{\sin\theta} & \theta_0 < \theta < \theta_B \\ r_h \frac{\sin\theta_h + \cos\theta_h \tan\beta}{\sin\theta + \tan\beta\cos\theta} & \theta_B < \theta < \theta_h \end{cases}$.

The internal energy dissipated along the failure surface can be expressed as follows:

$$D = \int_V cv \cos\varphi dL \tag{15}$$

and the infinitesimal surface element dL is calculated as follows:

$$dL = \frac{\rho}{\cos\varphi} \frac{R}{\sqrt{R^2 - (\rho - r_c)^2}} d\rho d\theta \tag{16}$$

Consequently, the internal energy dissipation can be expressed as follows:

$$D = c\omega \int_{\theta_0}^{\theta_h} \left[\int_{r_s}^{r} \rho^2 \frac{2R}{\sqrt{R^2 - (\rho - r_c)^2}} d\rho + br^2 \right] d\theta \tag{17}$$

Consequently, the energy balance equation [8] can be built and expressed as follows:

$$W_\gamma = D_{\text{int}} \tag{18}$$

Combining the strength reduction technique, the *FoS* of a 3D slope in disturbed rock masses can be derived from Equation (17) as follows:

$$FoS = f\left(\theta_0, \theta_h, r'_0/r_0 \middle| \sigma_{ci},\ GSI,\ m_i,\ D,\ \gamma,\ H,\ \beta,\ B/H\right) \tag{19}$$

Based on the strength reduction technique, the implicit expression of the *FoS* solution for a 3D slope in Equation (19) can be determined by the three independent variables θ_0, θ_h, and r'_0/r_0 with given strength parameters from the Generalized Hoek–Brown strength criterion. Thereafter, the upper bound—namely, a minimum *FoS* solution—can be obtained based on an optimization code using the exhaustion method: The optimization process changes a single variable one at a time to calculate the *FoS* solution with an increment of 0.01 for the three independent variables. By comparing the new *FoS* solution with the minimum result obtained from all of the previous computations, the minimum *FoS* solution can be captured.

5. Comparison

5.1. Comparison of FoS

In order to verify the validity of the present study, a comparison between the present 3D *FoS* solutions ($B \to \infty$) and the solutions by Li et al. [6] is conducted. In Table 1, the slope angle β = 30°, 45°, and 60°; GSI = 10, 30, 50, 70, and 100; and m_i = 5, 15, 25, and 35. FoS_0 is the solutions obtained by finite element lower bound analysis, and FoS_1, FoS_{02}, and FoS_{03} are the solutions obtained by Li et al. [6] based on Equations (5)–(7); Equations (5), (6) and (9); and Equations (5), (6) and (10), respectively.

It is seen from Table 1 that the existing *FoS* solutions, such as the FoS_2, the FoS_3, and the FoS_4 solutions, are either with a large error or only applicable for a small range of the inclined angle β of slope. The present 3D solutions under $B \to \infty$ are in good agreement with the existing 2D FoS_0 solutions, with a maximum error of 4.03% under β = 60°, GSI = 10, m_i = 35, and SR = 3.729. Consequently, the validity of the present work can be verified.

In the following analysis, the equivalent Mohr–Coulomb strength parameters method combining the upper bound theorem of limit analysis is employed to investigate the stability of a slope in disturbed rock masses.

Table 1. Comparison of present 3D *FoS* solutions with *FoS* solutions under 2D plane strain.

			Limit Analysis—Lower Bound		**SLIDE-Limit Equilibrium Using Equivalent Mohr–Coulomb Parameters**				**Limit Analysis**
			Nonlinear HB			**Equations (5)–(7)**	**Equations (5), (6) and (9)**	**Equations (5), (6) and (10)**	**Present 3D Solutions ($B \to \infty$)**
$\beta/°$	***GSI***	m_i	***SR***	FoS_0	FoS_1	FoS_2	FoS_3	FoS_4	FoS
30	100	5	0.070	1.0	1.014	0.988	-	1.0	0.9872
30	100	15	0.026	1.0	1.020	0.999	-	1.024	1.0243
30	100	25	0.016	1.0	1.023	1.003	-	1.036	1.0431
30	100	35	0.011	1.0	1.024	1.007	-	1.044	1.0327
30	70	5	0.218	1.0	1.018	0.985	-	1.011	1.0101
30	70	15	0.075	1.0	1.023	0.996	-	1.028	1.0202
30	70	25	0.045	1.0	1.024	1.004	-	1.035	1.0272
30	70	35	0.032	1.0	1.025	1.010	-	1.040	1.0306
30	50	5	0.461	1.0	1.020	0.993	-	1.014	1.0101
30	50	15	0.153	1.0	1.024	1.003	-	1.026	1.0171
30	50	25	0.091	1.0	1.025	1.024	-	1.032	1.0233
30	50	35	0.065	1.0	1.026	1.008	-	1.036	1.0302
30	30	5	1.057	1.0	1.022	1.001	-	1.012	1.0101
30	30	15	0.323	1.0	1.026	1.003	-	1.026	1.0162
30	30	25	0.185	1.0	1.026	1.005	-	1.031	1.0213
30	30	35	0.129	1.0	1.027	1.004	-	1.035	1.0278
30	10	5	4.363	1.0	1.023	1.002	-	1.006	1.0101
30	10	15	0.943	1.0	1.025	1.007	-	1.023	1.0168
30	10	25	0.460	1.0	1.026	0.996	-	1.033	1.0254
30	10	35	0.286	1.0	1.026	1.004	-	1.040	1.0316
45	100	5	0.135	1.0	1.000	1.008	1.022	1.027	0.9857
45	100	15	0.058	1.0	1.005	1.041	1.003	1.086	0.9886
45	100	25	0.036	1.0	1.012	1.047	1.003	1.110	0.9900
45	100	35	0.026	1.0	1.015	1.060	1.005	1.126	0.9900
45	70	5	0.469	1.0	1.001	1.038	1.001	1.055	0.9840
45	70	15	0.176	1.0	1.012	1.080	1.002	1.098	0.9900
45	70	25	0.108	1.0	1.017	1.060	1.007	1.113	0.9900
45	70	35	0.077	1.0	1.019	1.061	1.009	1.123	0.9900
45	50	5	1.046	1.0	1.004	1.045	1.001	1.063	0.9853
45	50	15	0.369	1.0	1.009	1.065	1.004	1.098	0.9900
45	50	25	0.222	1.0	1.020	1.066	1.010	1.110	0.9900
45	50	35	0.158	1.0	1.021	1.044	1.011	1.118	0.9900
45	30	5	2.593	1.0	1.011	1.066	0.999	1.060	0.9869
45	30	15	0.829	1.0	1.018	1.070	1.007	1.094	0.9900
45	30	25	0.480	1.0	1.021	1.074	1.010	1.110	0.9900
45	30	35	0.334	1.0	1.024	1.085	1.011	1.118	1.0101
45	10	5	13.585	1.0	1.014	1.087	1.000	1.039	0.9847
45	10	15	3.155	1.0	1.023	1.106	1.005	1.080	0.9900
45	10	25	1.552	1.0	1.023	1.107	1.009	1.103	0.9900
45	10	35	0.969	1.0	1.026	1.079	1.010	1.115	0.9900
60	100	5	0.232	1.0	1.001	1.033	1.043	-	0.9822
60	100	15	0.130	1.0	1.004	1.114	1.026	-	1.0101
60	100	25	0.088	1.0	1.004	1.146	1.035	-	1.0155
60	100	35	0.066	1.0	1.004	1.141	1.040	-	1.0241
60	70	5	0.946	1.0	1.013	1.059	1.024	-	0.9891
60	70	15	0.435	1.0	1.004	1.143	1.033	-	1.0153
60	70	25	0.276	1.0	1.004	1.161	1.043	-	1.0252
60	70	35	0.20	1.0	1.005	1.183	1.047	-	1.0284
60	50	5	2.337	1.0	1.005	1.124	1.026	-	0.9900
60	50	15	0.953	1.0	1.004	1.171	1.036	-	1.0201
60	50	25	0.584	1.0	1.008	1.176	1.046	-	1.0267
60	50	35	0.419	1.0	1.009	1.172	1.049	-	1.0302

Table 1. *Cont.*

			Limit Analysis—Lower Bound		SLIDE-Limit Equilibrium Using Equivalent Mohr–Coulomb Parameters				Limit Analysis
			Nonlinear HB			Equations (5)–(7)	Equations (5), (6) and (9)	Equations (5), (6) and (10)	Present 3D Solutions ($B \to \infty$)
$\beta/°$	GSI	m_i	SR	FoS_0	FoS_1	FoS_2	FoS_3	FoS_4	FoS
60	30	5	6.439	1.0	1.009	1.150	1.023	-	1.0101
60	30	15	2.317	1.0	1.009	1.197	1.044	-	1.0239
60	30	25	1.356	1.0	1.010	1.201	1.049	-	1.0294
60	30	35	0.945	1.0	1.011	1.230	1.051	-	1.0319
60	10	5	38.926	1.0	1.004	1.183	1.013	-	0.9900
60	10	15	11.734	1.0	1.013	1.257	1.048	-	1.0288
60	10	25	5.928	1.0	1.017	1.261	1.054	-	1.0366
60	10	35	3.729	1.0	1.018	1.258	1.059	-	1.0403

5.2. Validity of Index SR

It has been proved that for rock slopes in undisturbed rock masses (D = 0) with a given slope angle β, GSI, and m_i, the FoS of a slope in Hoek–Brown media is only related to SR = $\sigma_{ci}/\gamma H$. In the present study, validity of index SR for slopes in disturbed rock mass is investigated, as shown in Table 2 [11]. It is known from Table 2 that the FoS of a disturbed slope in Hoek–Brown media is still only related to index SR with given β, GSI, m_i, and D. In other words, the FoS of a 3D Hoek–Brown slope in disturbed rock mass can be described as follows:

$$FoS = f\left(\theta_0,\ \theta_h,\ r'_0/r_0,\ B/H \middle|\ SR,\ GSI,\ m_i,\ \beta,\ \ D\right) \tag{20}$$

Table 2. FoS of slope in rock mass under different cases with the same SR [11].

Input Parameters	Case 1	Case 2	Case 3
GSI	30	30	30
m_i	8	8	8
$\beta/°$	60	60	60
σ_{ci}/kPa	20	25	250
$\gamma/(\mathrm{kN/m^3})$	23	28.75	23.96
H/m	25	25	300
SR ($\sigma_{ci}/\gamma H$)	34.783	34.783	34.783
FoS (D = 0)			
Bishop simplified	2.026	2.026	2.026
Janbu simplified	1.934	1.934	1.934
Spencer	2.032	2.032	2.032
Morgenstern–Price	2.027	2.027	2.027
Phase^2 8.0 (FEM)	2.000	2.040	2.030
Present 3D solution ($B \to \infty$)			
D = 0	2.0230	2.0230	2.0229
D = 0.3	1.7066	1.7066	1.7066
D = 0.7	1.2477	1.2477	1.2477
D = 1.0	0.8416	0.8416	0.8416

6. Results and Discussion

6.1. Parametric Analysis of the Disturbance Factor D on Slope Stability

A parametric analysis is conducted to investigate the effects of disturbance factor D on the stability of a 3D slope in rock masses. As shown in Figure 4a, B/H has a significant impact on slope stability that FoS decreases sharply with the increase in B/H within $0 < B/H \leq 2.0$ and thereafter reaches a constant value asymptotically. It is illustrated that a 3D stability analysis of slope is essential, especially for slopes of which the width is limited. From Figure 4b, it is clear that the *FoS* decreases more than 60% linearly when the disturbance factor *D* increases from 0 to 1.0, namely, the disturbance factor *D* is a non-negligible factor for slope stability and should be considered in the stability analysis of slopes in rock masses.

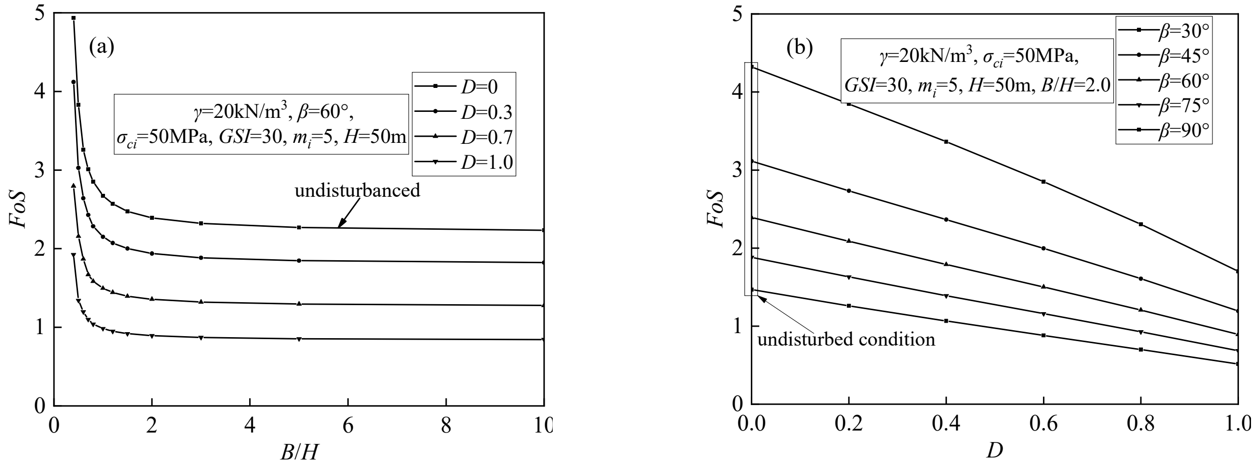

Figure 4. Effects of rock mass disturbance on stability of slope in Hoek–Brown media and (**a**) B/H = 0~10 with different D; (**b**) D = 0~1.0 with different β.

6.2. Design Charts for 3D Rock Slopes

Commercial software provides a convenient way to estimate the *FoS* of slopes. However, at the present time, most of the commercial software is still programmed using the linear Mohr–Coulomb failure criterion, ignoring the nonlinear strength character of rock masses. Stability charts are still a convenient and powerful tool to estimate *FoS* solutions of slope in rock masses [6–8,10–14]. Existing chart-based stability analysis of rock slopes was mainly conducted under 2D plane strain [6,7,10–14]. However, it is clear from Figure 4 that the 3D character of slope is a dominating factor on *FoS* solutions of slope. It is of theorical and practical importance to investigate 3D stability of rock slope and to present stability charts of 3D disturbed rock mass slopes in Hoek–Brown media. From this point of view, a set of stability charts of 3D slope with slope angle β = 45° in disturbed rock masses with ratio B/H = 0.7, 1.0, 1.2, 1.5, 2.0, and 5.0, and D = 0, 0.3, 0.7, and 1.0, are proposed in Figures 5–8. The Hoek–Brown strength parameters in the stability charts are $10 \le GSI \le 100$ and $5 \le m_i \le 35$.

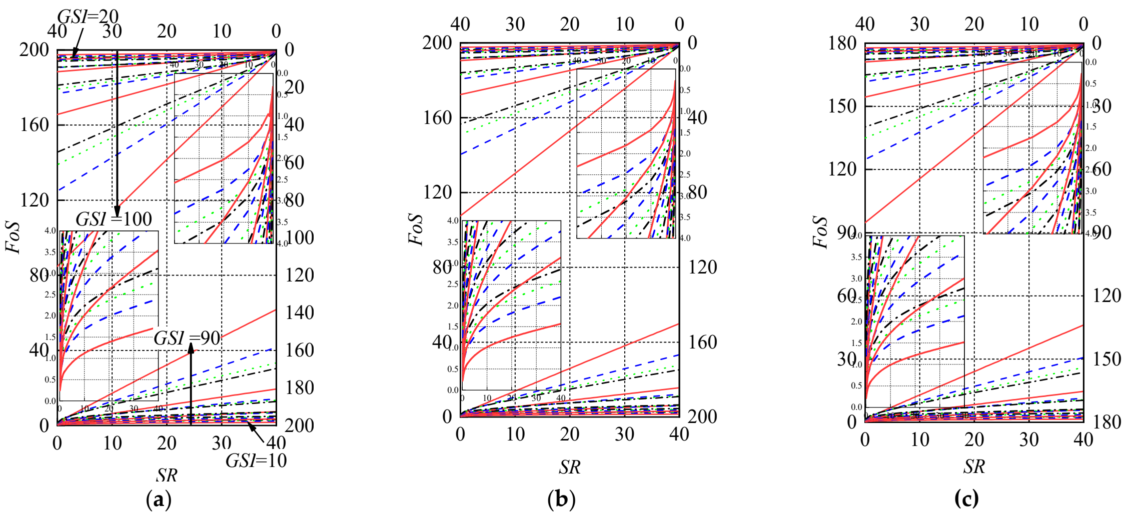

Figure 5. *Cont.*

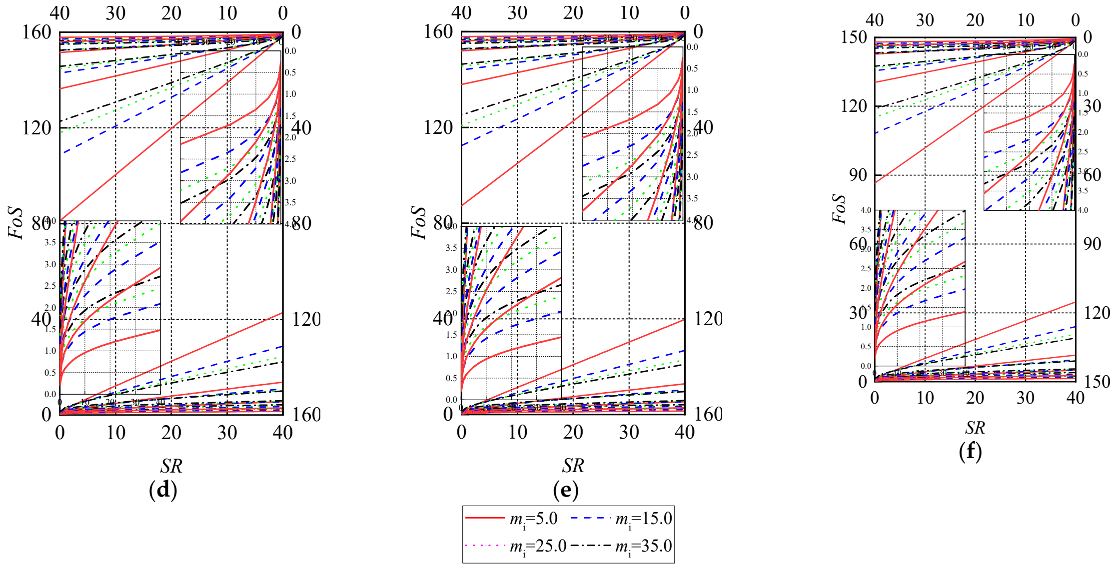

Figure 5. Stability charts of slope in Hoek–Brown media with $D = 0$ (undisturbed) and (**a**) $B/H = 0.7$; (**b**) $B/H = 1.0$; (**c**) $B/H = 1.2$; (**d**) $B/H = 1.5$; (**e**) $B/H = 2.0$; (**f**) $B/H = 5.0$.

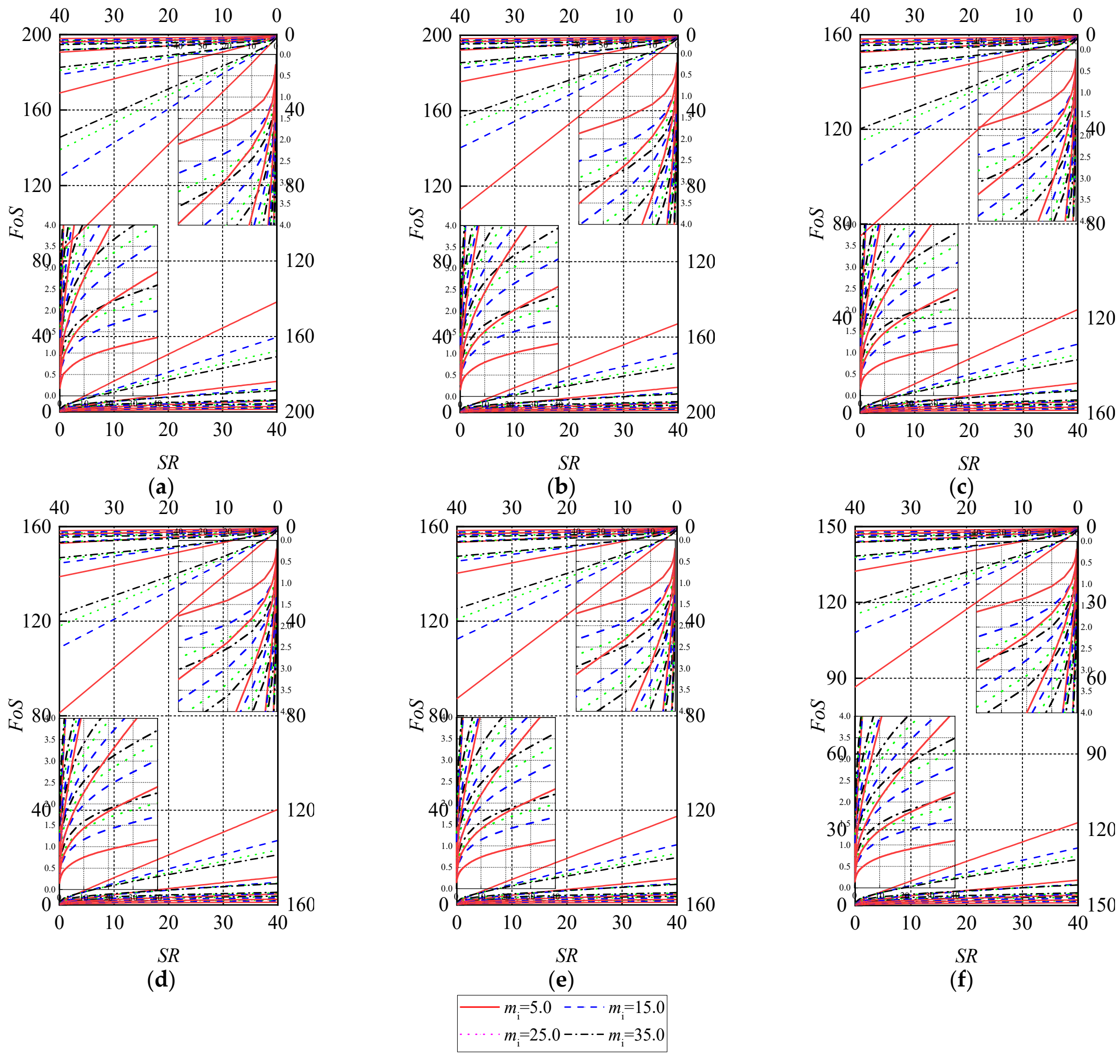

Figure 6. Stability charts of slope in Hoek–Brown media with $D = 0.3$ and (**a**) $B/H = 0.7$; (**b**) $B/H = 1.0$; (**c**) $B/H = 1.2$; (**d**) $B/H = 1.5$; (**e**) $B/H = 2.0$; (**f**) $B/H = 5.0$.

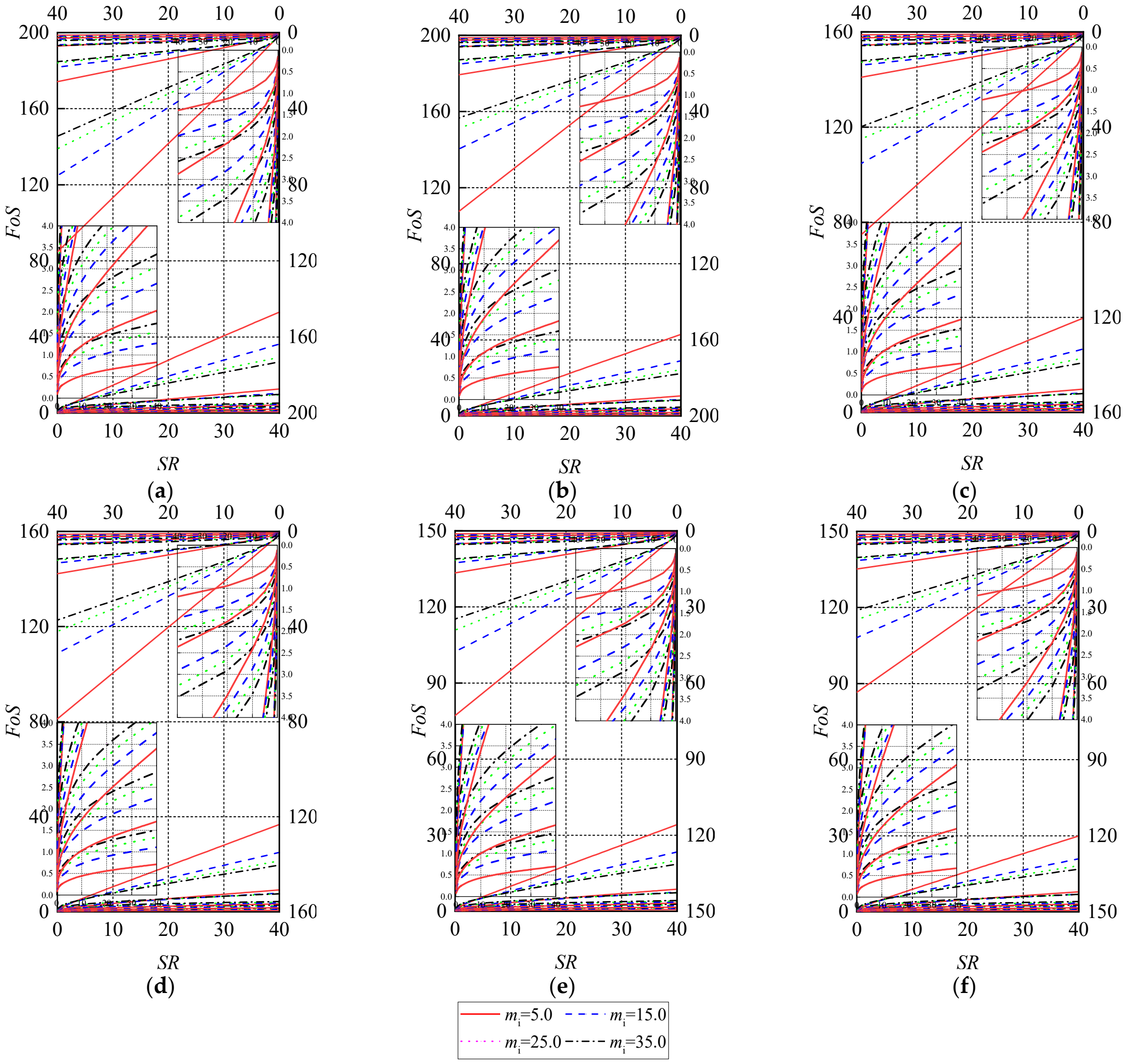

Figure 7. Stability charts of slope in Hoek–Brown media with D = 0.7 and (**a**) B/H = 0.7; (**b**) B/H = 1.0; (**c**) B/H = 1.2; (**d**) B/H = 1.5; (**e**) B/H = 2.0; (**f**) B/H = 5.0.

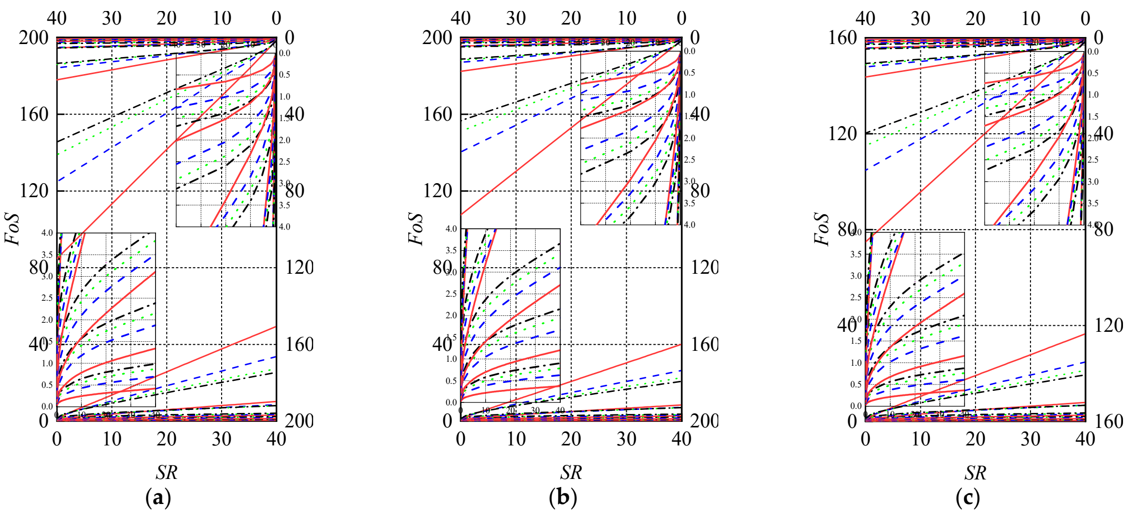

Figure 8. *Cont.*

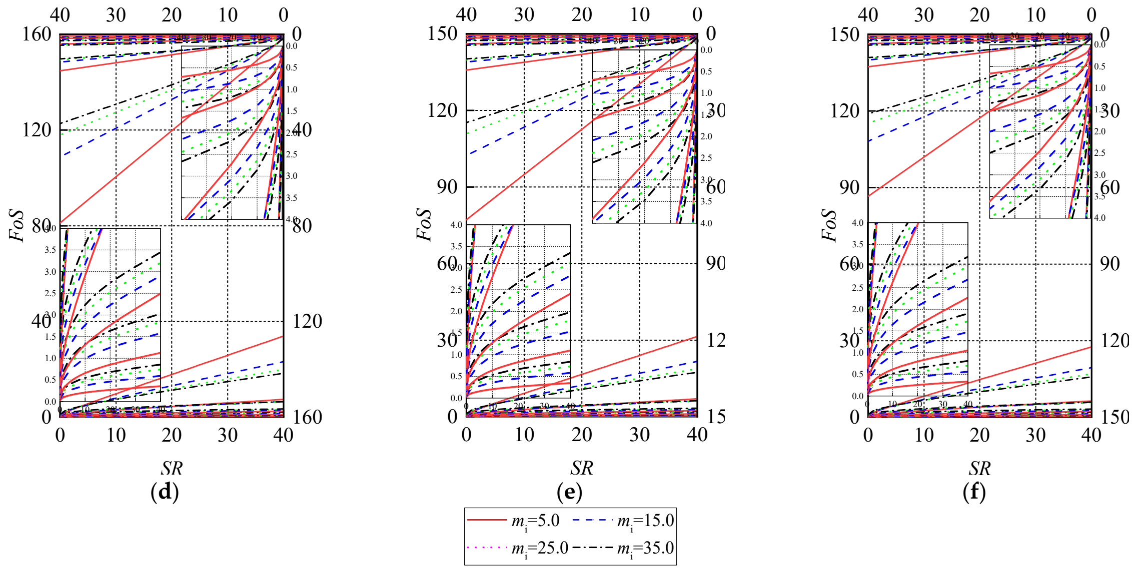

Figure 8. Stability charts of slope in Hoek–Brown media with D = 1.0 and (**a**) B/H = 0.7; (**b**) B/H = 1.0; (**c**) B/H = 1.2; (**d**) B/H = 1.5; (**e**) B/H = 2.0; (**f**) B/H = 5.0.

It can be seen from Figures 5–8 that the *FoS* solutions first show a nonlinear then a linear rule versus the index SR. Besides, it is also clear that the index *SR*, the strength parameter *GSI*, and the ratio B/H have positive effects, while the strength parameter m_i, the slope angle β, and the rock mass disturbance factor D have negative effects, on the stability of a 3D rock slope. Besides, Figures 5–8 provide a convenient and straightforward approach to obtain the *FoS* solutions of rock slopes. Once the slope geometric characteristics—that is, the height, the width, and the inclined angle of the slope—and the strength parameters—namely, σ_{ci}, *GSI*, m_i, and D—the *FoS* solution of a 3D slope can be obtained from Figures 5–8 directly. The application examples for the design charts in Figures 5–8 can be seen in Section 7 Case Study.

6.3. The Slope Angle Weighting Factor f_{β_3D} for 3D Slopes

Besides the design charts, the curve-fitting equations make up another effective methodology to calculate the *FoS* solutions easily, such as the slope angle weighting factor f_β equations proposed by Shen et al. [11] and Sun et al. [12] for 2D slopes. In this work, to develop the weighting factor from 2D plane strain to 3D cases, the validity of the 2D slope angle weighting factor f_β equations is examined firstly, as shown in Table 3 and Figure 9. Thereafter, the weighting factor f_β can be modified from 2D to 3D cases.

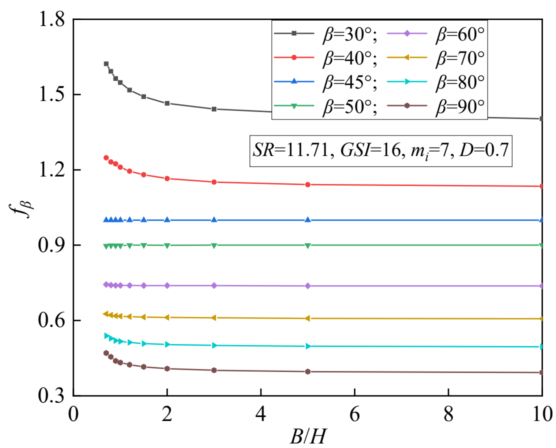

Figure 9. Slope angle weighting factor f_β versus B/H.

Table 3. Comparison of slope angle weight factor f_β with Shen et al. [11] and Sun et al. [12].

H/m	β/°	γ/ (kN/m^3)	σ_{ci}/ kPa	GSI	m_i	D	f_β Shen et al. [11]	Sun et al. [12]	Present solution B/H =0.7	B/H =1.0	B/H →∞
184	55	27	153	47	9	0.9	0.793	0.817	0.825	0.827	0.828
140	34	26	50	28	8	0.7	1.259	1.264	1.439	1.389	1.290
220	45	27	65	44	17	0.8	1.000	1.000	1.000	1.000	1.000
135	65	27	172	58	9	0.9	0.637	0.753	0.734	0.732	0.733
70	50	27	29	41	7	0.8	0.885	0.901	0.905	0.903	0.905
110	45	26.5	50	25	10	0.7	1.000	1.000	1.000	1.000	1.000
270	45	27	109	39	18	0.9	1.000	1.000	1.000	1.000	1.000
170	55	30	104	48	7	0.7	0.793	0.814	0.830	0.828	0.831
60	60	27	65	44	13	1.0	0.711	0.710	0.754	0.752	0.751
35	67	27	109	28	12	1.0	0.609	0.571	0.664	0.659	0.651
63	35	27	109	28	12	1.0	1.232	1.252	1.361	1.326	1.256
70	49	27	3	49	25	1.0	0.905	0.941	0.921	0.920	0.922
58	50	27	5	55	22	1.0	0.885	0.922	0.900	0.902	0.904
60	48	27	5	54	22	1.0	0.925	0.944	0.937	0.939	0.940
60	52	27	5	56	22	1.0	0.847	0.930	0.865	0.868	0.869
40	71	27	50	33	14	1.0	0.558	0.538	0.621	0.614	0.602
110	50	27	50	25	14	1.0	0.885	0.903	0.899	0.900	0.901
41	50	27	3	46	24	1.0	0.885	0.899	0.900	0.902	0.904
41	55	27	3	49	24	1.0	0.793	0.848	0.820	0.819	0.820
46	55	27	3	50	24	1.0	0.793	0.810	0.820	0.819	0.821
57	49	27	3	48	24	1.0	0.905	0.909	0.921	0.921	0.922
57	37	27	3	48	24	1.0	1.179	1.185	1.374	1.328	1.221
57	40	27	3	48	24	1.0	1.103	1.130	1.288	1.246	1.154
57	42	27	3	48	24	1.0	1.056	1.083	1.235	1.198	1.113
27	45	25	0.75	100	10	0	1.000	1.000	1.000	1.000	1.000
50	60	23	10	30	8	1.0	0.711	0.722	0.746	0.746	0.745
50	45	27	13.5	30	5	0.7	1.000	1.000	1.000	1.000	1.000
25	45	27	5.4	20	20	0.7	1.000	1.000	1.000	1.000	1.000
5	30	27	2.7	10	5	0.5	1.375	1.438	1.615	1.551	1.433
25	75	25	0.625	80	15	0.3	0.511	0.525	0.605	0.591	0.577
250	60	23	46	50	35	1.0	0.711	0.652	0.746	0.745	0.743

It is shown in Table 3 and Figure 9 that, for slopes within the range of 45° to 60°, the slope angle weight factor f_β is barely influenced by B/H. However, with regard to slopes within the range of $30° \leq \beta < 45°$ and $60° < \beta \leq 90°$, there is a significant influence of B/H on f_β. It is also seen that the when $30° \leq \beta < 45°$ and $60° < \beta \leq 90°$, the ratio f_{β_3D}/f_β varies with B/H significantly. In other words, it is necessary to take into account B/H on the estimation of f_{β_3D}. As a result, the curve-fitting strategy is employed to determine the estimation equations to estimate the slope angle weighting factor f_{β_3D} considering the influence of B/H, as listed in Table 4.

Table 4. Modified equations to estimate the slope angle weighting factor f_{β_3D} of 3D slope ($0 \leq FoS \leq 4$).

B/H	Regression Equations—$f_{\beta\_B/H}$	Fitting Degree—R^2
0.7	$35.7\,\beta^{-0.9091}$, $30° \leq \beta < 45°$ $62.2\,\beta^{-1.082}$, $45° < \beta \leq 90°$	0.9992 0.9995
1.0	$28.52\,\beta^{-0.8569}$, $30° \leq \beta < 45°$ $2.26\,e^{-0.01849\beta}$, $45° < \beta \leq 90°$	0.9997 0.9993
1.2	$26.04\,\beta^{-0.8355}$, $30° \leq \beta < 45°$ $2.301\,e^{-0.01882\beta}$, $45° < \beta \leq 90°$	0.9998 0.9996
1.5	$23.91\,\beta^{-0.816}$, $30° \leq \beta < 45°$ $2.342\,e^{-0.01914\beta}$, $45° < \beta \leq 90°$	0.9994 0.9998
2.0	$22.38\,\beta^{-0.8012}$, $30° \leq \beta < 45°$ $2.382\,e^{-0.01945\beta}$, $45° < \beta \leq 90°$	0.9998 0.9998
5.0	$19.85\,\beta^{-0.7745}$, $30° \leq \beta < 45°$ $2.442\,e^{-0.01994\beta}$, $45° < \beta \leq 90°$	0.9999 0.9996

Consequently, the *FoS* solution of a 3D slope can be expressed as follows:

$$FoS = FoS_{45^\circ} \times f_{\beta\_3D} \tag{21}$$

7. Case Study

In order to explain how the proposed stability charts and the modified equations can be applied to engineering practice, two cases—that is, a rock slope of an open pit mine at Baskoyak Anatolia and a rock slope in Kisrakdere coal open pit mine in western Turkey—are introduced and analyzed as follows.

7.1. A Rock Slope of an Open Pit Mine at Baskoyak Anatolia

A case study was conducted to apply the present *FoS* solutions to practical issues. As reported by Sun et al. [12] and Li et al. [13], a rock slope of an open pit mine at Baskoyak Anatolia is selected as the first case. Due to the heavily joint nature of rock mass, the slope was assumed to be homogeneous and isotropic [27]. The height and angle of the slope are H = 20 m and β = 34°, respectively; average value of unit weight γ = 22.2 kN/m^3; and uniaxial compressive strength σ_{ci} = 5.2 MPa. The Hoek–Brown strength parameters are m_i = 7, GSI = 16, and disturbance factor D = 0.7; the related parameters for the first case and calculated *FoS* are summarized in Table 5 [12].

Table 5. *FoS* solutions of slopes from case study.

Input Parameters		Case 1	Case 2
$\beta/^\circ$		34	60
GSI		16	37
m_i		7	9.04
D		0.7	1.0
σ_{ci}/MPa		5.2	40
γ/(kN/m^3)		22.2	21
H/m		20	80
SR		11.71	23.81
FoS	Li et al. [6]	0.90	1.13
	Shen et al. [11]	0.95	1.22
	Sun et al. [12]	0.93	1.06
	ABAQUS by Sun et al. [12]	0.97	1.14
Present 3D solutions	B/H = 5.0 from present charts	0.92	0.99
	$B/H\to\infty$	0.89	0.98

The process to use the stability charts to estimate the *FoS* of slope is as follows: First, a linear interpolation is employed between the curves of GSI = 10 and GSI = 20 based on Figure 7a to determine $FOS_{\beta\ =\ 45^\circ}$ = 0.86 for m_i = 7 under B/H = 0.7. Second, $FOS_{\beta=34^\circ}$ = 0.86 × 35.7 × 34$^{-0.9091}$ = 1.25 is obtained using the estimating equation listed in Table 5. Third, Figure 7b–f are used to determine *FoS* solutions under B/H = 1.0, B/H = 1.2, B/H = 1.5, B/H =2.0, and B/H = 5.0, as shown in Table 5 and Figure 10.

7.2. A Rock Slope in Kisrakdere Coal Open Pit Mine in Western Turkey

The other case selected for the case study is a homogeneous and isotropic rock slope of the Kisrakdere coal mine in the Soma lignite Basin, Turkey [12,13]. The height and angle of slope are H = 80 m and β = 60°, respectively. Average unit weight of rock mass γ = 21 kN/m^3, and uniaxial compressive strength of rock mass σ_{ci} = 40 MPa. The Hoek–Brown strength parameters are GSI = 37, m_i = 9.04 and D = 1.0. The parameters for the analysis of Case 2 and *FoS* obtained in virtue of the proposed charts are also listed in Table 5. The calculation process is: $FOS_{\beta=45^\circ}$ = 1.69 under GSI = 37, m_i = 9.04, D = 1.0 and B/H = 0.7 is obtained based on Figure 8a. Second, $FOS_{\beta=60^\circ}$ = 1.69 × 62.2 × 60$^{-1.082}$ = 1.25 is obtained using Table 5. Third, a series of *FoS* solutions under various B/H = 1.0, B/H = 1.2, B/H = 1.5, B/H = 2.0, and B/H = 5.0, are obtained, as shown in Table 5 and Figure 10.

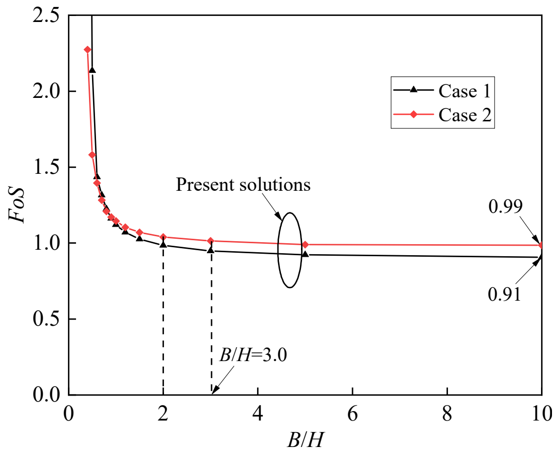

Figure 10. *FoS* solution of slope from case study under 3D condition.

It can be seen from Table 5 that the present 3D solutions are in good agreement with the previous *FoS* solutions. It should be noted that the previous *FoS* solutions were obtained under 2D plane strain, and it is clear from Figure 10 that ratio B/H has a significant impact on *FoS* solutions. When the width of the failure block is greater than slope height ($B/H \geq 2.0$), *FoS* solutions under 2D plane strain will be adequate; however, for conditions where the width of slope is limited ($B/H < 2.0$), a 3D stability analysis will be more appropriate and advanced to estimate the *FoS* solutions of slope.

8. Conclusions

Based on the upper bound theorem of limit analysis, this study presents a chart-based stability analysis to investigate the stability of a 3D slope in disturbed rock masses following the Generalized Hoek–Brown failure criterion. Analytical expression of the *FoS* of 3D slope is proposed in virtue of the strength reduction technique, and a set of stability charts for slope are proposed based on the index $SR = \sigma_{ci}/\gamma H$. Modified equations to estimate the slope angle weight factor $f_{\beta\_3\mathrm{D}}$ are proposed to build a fast and convenient method to solve the *FoS* of 3D slopes. A case study is conducted to apply the present stability charts on practical cases. The main conclusions of the present study can be drawn as follows:

1. Validities of the present study and index *SR* on estimating the *FoS* solutions of a 3D slope in disturbed rock masses are verified that for a slope with given B/H; slope angle β; and Hoek–Brown strength parameters *GSI*, m_i, and *D*, the *FoS* of slope is still only related to index *SR*.
2. A parametric analysis is conducted to investigate the effects of 3D character and rock mass disturbance on slope stability. It is shown that B/H and the rock mass disturbance factor *D* have significant influences on slope stability and should be considered in stability analyses of slopes in rock masses.
3. A series of stability charts are presented and modified equations to determine the slope angle weighting factor $f_{\beta\_3\mathrm{D}}$ considering the 3D character of slope are presented to provide a convenient and straightforward way to estimate *FoS* solutions of 3D slopes in disturbed rock masses.
4. A case study is conducted to apply the presented stability charts to practical cases. The results indicated that the present *FoS* solutions obtained using the stability charts in conjunction with the slope angle weighting factor $f_{\beta\_3\mathrm{D}}$ are in good agreement with the analytical solutions. The validity of the present stability charts and the equations to estimate the slope angle weighting factors $f_{\beta\_3\mathrm{D}}$ are verified.

Author Contributions: J.X., methodology, validation, formal analysis, data curation, writing—original draft, and visualization. X.W., validation, formal analysis, data curation, and writing—original draft. P.X., validation, formal analysis, data curation, writing—original draft. R.W., validation, formal analysis, data curation, and writing—original draft. D.D., writing and visualization. All authors have read and agreed to the published version of the manuscript.

Funding: This work was supported by the National Natural Science Foundation of China (52208327, 52108305), the Natural Science Foundation of Jiangsu Province (BK20210256), and the Fundamental Research Funds for the Central Universities (2242022k30030 and 2242022k30031).

Data Availability Statement: The datasets in the current study are available from the corresponding author on reasonable request. The data are not publicly available due to privacy.

Acknowledgments: The financial support is greatly appreciated.

Conflicts of Interest: The authors declare that they have no known competing financial interests or personal relationships that could have appeared to influence the work reported in this paper.

References

1. Hoek, E.; Brown, E.T. Empirical strength criterion for rock masses. *J. Geotech. Eng. Div. ASCE* **1980**, *106*, 1013–1035. [CrossRef]
2. Hoek, E.; Carranza-Torres, C.; Corkum, B. Hoek–Brown failure criterion-2002 edition. *Proc. NARMS-Tac* **2002**, *1*, 267–273.
3. Yang, X.L. Effect of Pore-Water Pressure on 3D stability of rock slope. *Int. J. Geomech.* **2017**, *17*, 06017015. [CrossRef]
4. Pan, Q.J.; Jiang, Y.J.; Dias, D. Probabilistic stability analysis of a three-dimensional rock slope characterized by the Hoek-Brown failure criterion. *J. Comput. Civ. Eng.* **2017**, *31*, 04017046. [CrossRef]
5. Qin, C.B.; Chian, S.C.; Wang, C.Y. Kinematic analysis of pile behavior for improvement of slope stability in fractured and saturated Hoek-Brown rock masses. *Int. J. Numer. Anal. Methods Geomech.* **2017**, *41*, 803–827. [CrossRef]
6. Li, A.J.; Merifield, R.S.; Lyamin, A.V. Stability charts for rock slopes based on the Hoek–Brown failure criterion. *Int. J. Rock Mech. Min. Sci.* **2008**, *45*, 689–700. [CrossRef]
7. Li, A.J.; Lyamin, A.V.; Merifield, R.S. Seismic rock slope stability charts based on limit analysis methods. *Comput. Geotech.* **2009**, *36*, 135–148. [CrossRef]
8. Xu, J.S.; Yang, X.L. Seismic stability analysis and charts of a 3D rock slope in Hoek–Brown media. *Int. J. Rock Mech. Min. Sci.* **2018**, *112*, 64–76. [CrossRef]
9. Saada, Z.; Maghous, S.; Garnier, D. Stability analysis of rock slopes subjected to seepage forces using the modified Hoek–Brown criterion. *Int. J. Rock Mech. Min. Sci.* **2012**, *55*, 45–54. [CrossRef]
10. Jiang, X.Y.; Cui, P.; Liu, C.Z. A chart-based seismic stability analysis method for rock slopes using Hoek–Brown failure criterion. *Eng. Geol.* **2016**, *209*, 196–208. [CrossRef]
11. Shen, J.Y.; Karakus, M.; Xu, C.S. Chart–based slope stability assessment using the Generalized Hoek–Brown criterion. *Int. J. Rock Mech. Min. Sci.* **2013**, *64*, 210–219. [CrossRef]
12. Sun, C.W.; Chai, J.R.; Xu, Z.G.; Qin, Y.; Chen, X.Z. Stability charts for rock mass slopes based on the Hoek–Brown strength reduction technique. *Eng. Geol.* **2016**, *214*, 94–106. [CrossRef]
13. Li, A.J.; Merifield, R.S.; Lyamin, A.V. Effect of rock mass disturbance on the stability of rock slopes using the Hoek–Brown failure criterion. *Comput. Geotech.* **2011**, *38*, 546–558. [CrossRef]
14. Li, A.J.; Qian, Z.G.; Jiang, J.C.; Lyamin, A. Seismic slope stability evaluation considering rock mass disturbance varying in the slope. *KSCE J. Civ. Eng.* **2019**, *23*, 1043–1054. [CrossRef]
15. Park, D. Measures of slope stability in bonded soils governed by linear failure criterion with tensile strength cut-off. *Comput. Geotech.* **2023**, *161*, 105610. [CrossRef]
16. Michalowski, R.L.; Park, D. Stability assessment of slopes in rock governed by the Hoek-Brown strength criterion. *Int. J. Rock Mech. Min. Sci.* **2020**, *127*, 104217. [CrossRef]
17. Park, D.; Michalowski, R.L. Three-dimensional stability assessment of slopes in intact rock governed by the Hoek-Brown failure criterion. *Int. J. Rock Mech. Min. Sci.* **2021**, *137*, 104522. [CrossRef]
18. Xu, J.S.; Du, X.L. Seismic stability of 3D rock slopes based on a multi-cone failure mechanism. *Rock Mech. Rock Eng.* **2023**, *56*, 1595–1605. [CrossRef]
19. Hu, Y.N.; Ji, J.; Sun, Z.B.; Dias, D. First order reliability-based design optimization of 3D pile-reinforced slopes with Pareto optimality. *Comput. Geotech.* **2023**, *162*, 105635. [CrossRef]
20. Sun, Z.; Zhao, Y.; Hu, Y.; Dias, D.; Ji, J. Probabilistic analysis of width-limited 3D slope in spatially variable soils: UBLA enhanced with efficiency-improved discretization of horn-like failure mechanism. *Int. J. Numer. Anal. Methods Geomech.* **2023**, *47*, 3129–3157. [CrossRef]
21. Michalowski, R.L. Three-dimensional stability of slopes and excavations. *Geotechnique* **2009**, *59*, 839–850. [CrossRef]
22. Gao, Y.F.; Zhang, F.; Lei, G.H.; Li, D.Y.; Wu, Y.X.; Zhang, N. Stability charts for 3D failures of homogeneous slopes. *J. Geotech. Geoenviron. Eng.* **2013**, *139*, 1528–1538. [CrossRef]

23. Gao, Y.F.; Zhu, D.S.; Zhang, F.; Lei, G.H.; Qin, H.Y. Stability analysis of three-dimensional slopes under water drawdown conditions. *Can. Geotech. J.* **2014**, *51*, 1355–1364. [CrossRef]
24. Pérez-Reya, I.; Alejanoa, L.R.; Riquelmeb, A.; González-deSantosa, L. Failure mechanisms and stability analyses of granitic boulders focusing a case study in Galicia (Spain). *Int. J. Rock Mech. Min. Sci.* **2019**, *119*, 58–71. [CrossRef]
25. Zhang, J.H.; Wang, W.J.; Zhang, D.B.; Zhang, B.; Meng, F. Safe range of retaining pressure for three-dimensional face of pressurized tunnels based on limit analysis and reliability method. *KSCE J. Civ. Eng.* **2018**, *22*, 4645–4656. [CrossRef]
26. Huang, F.; Zhao, L.H.; Ling, T.H.; Yang, X.L. Rock mass collapse mechanism of concealed karst cave beneath deep tunnel. *Int. J. Rock Mech. Min. Sci.* **2017**, *91*, 133–138. [CrossRef]
27. Sonmez, H.; Ulusay, R. Modifications to the geological strength index (GSI) and their applicability to stability of slopes. *Int. J. Rock Mech. Min. Sci.* **1999**, *36*, 743–760. [CrossRef]

Disclaimer/Publisher's Note: The statements, opinions and data contained in all publications are solely those of the individual author(s) and contributor(s) and not of MDPI and/or the editor(s). MDPI and/or the editor(s) disclaim responsibility for any injury to people or property resulting from any ideas, methods, instructions or products referred to in the content.